The ins and outs of ligand binding to CCR2

Zweemer, A.J.M.

Citation

Version:	Corrected Publisher's Version
License:	[Licence agreement concerning inclusion of doctoral thesis in the Institutional Repository of the University of Leiden](#)
Downloaded from:	[https://hdl.handle.net/1887/29763](#)

Cover Page

The handle http://hdl.handle.net/1887/29763 holds various files of this Leiden University dissertation

Author: Zweemer, Annelien
Title: The ins and outs of ligand binding to CCR2
Issue Date: 2014-11-20

Chapter 6

Structure-Kinetics Relationships – an overlooked parameter in hit-to-lead optimization: a case of cyclopentylamines as CCR2 antagonists

Maris Vilums*

Annelien J.M. Zweemer*

Zhiyi Yu

Henk de Vries

Julia M. Hillger

Hannah Wapenaar

Ilse A.E. Bollen

Farhana Barmare

Raymond Gross

Jeremy Clemens

Paul Krenitsky

Johannes Brussee

Dean Stamos

John Saunders

Laura H. Heitman

Adriaan P. IJzerman

*These authors contributed equally

Abstract

Preclinical models of inflammatory diseases (e.g., neuropathic pain, rheumatoid arthritis, and multiple sclerosis) have pointed to a critical role of the chemokine receptor 2 (CCR2) and chemokine ligand 2 (CCL2). However, one of the biggest problems of high-affinity inhibitors of CCR2 is their lack of efficacy in clinical trials. We report a new approach for the design of high-affinity and long-residence-time CCR2 antagonists. We developed a new competition association assay for CCR2, which allows us to investigate the relation of the structure of the ligand and its receptor residence time (i.e., structure–kinetic relationship (SKR)) next to a traditional structure–affinity relationship (SAR). By applying combined knowledge of SAR and SKR, we were able to re-evaluate the hit-to-lead process of cyclopentylamines as CCR2 antagonists. Affinity-based optimization yielded compound **1** with good binding (K_i = 6.8 nM) but very short residence time (2.4 min). However, when the optimization was also based on residence time, the hit-to-lead process yielded compound **22a**, a new high-affinity CCR2 antagonist (3.6 nM), with a residence time of 135 min.

Introduction

Chemokines are a class of chemoattractant cytokines, and their main action is to control the trafficking and activation of leukocytes and other cell types for a range of inflammatory and non-inflammatory conditions. One of these, monocyte chemotactic protein-1 (MCP-1/ chemokine ligand 2 (CCL2)), acts on monocytes, memory T cells, and basophils [1]. It creates a chemotactic gradient and activates the movement of immune cells to the site of inflammation by binding to its cell-surface receptor, chemokine receptor 2 (CCR2) [2]. This CCL2/CCR2 pair is overexpressed in several inflammatory conditions, in which excessive monocyte recruitment is observed. CCR2 and CCL2 knockout mice and CCR2 or CCL2 antibody-treated rodents show decreased recruitment of monocytes and produce considerably decreased inflammatory responses [3]. This indicates CCR2 as a potential target for the treatment of several immune-based inflammatory diseases and conditions, such as multiple sclerosis [4], atherosclerosis [5], rheumatoid arthritis [6], diabetes [7], asthma [8], and neuropathic pain [9].

In the past decade, there has been an increasing interest in the development of small-molecule antagonists of the CCR2 receptor, resulting in the disclosure of many different chemical classes. However, there are still no selective CCR2 antagonists on the market for the treatment of inflammatory diseases. Clinical trials, thus far, have failed mostly because of the lack of efficacy, including the one for the CCR2 antagonist MK-0812 (Fig. 1) [10].
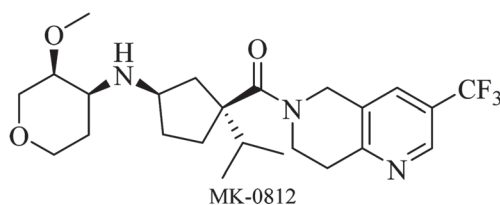

Fig. 1. CCR2 antagonist MK-0812

It has been suggested that binding kinetics, especially the lifetime of the ligand–receptor complex, can be used as a predictor for drug efficacy and safety [11, 12]. The concept of binding kinetics is often overlooked in the early phase of drug discovery; however, incorporation of this parameter could help to decrease the attrition rate in later stages of drug development [13]. In this concept of kinetics, an additional pharmacological parameter, the ligand–receptor residence time (RT; the reciprocal of the dissociation rate constant k_{off}), is defined [14], which is a measure for the duration that a ligand is bound to its target.

In this study, we first evaluated several reference CCR2 antagonists using a recently developed competition association assay for CCR2 that yielded the respective association and dissociation rate constants. As our starting point, we chose compound **1**, which was also the lead compound in the process that led to the development of MK-0812 by the Merck group [10]. The determination of the binding kinetics of several known structures with this particular scaffold subsequently allowed us to generate a new series of high-affinity and long-residence-time CCR2 antagonists based on structure **2**, which was previously abandoned by other groups in optimization steps because of its modest binding affinity (Fig. 2) [15].
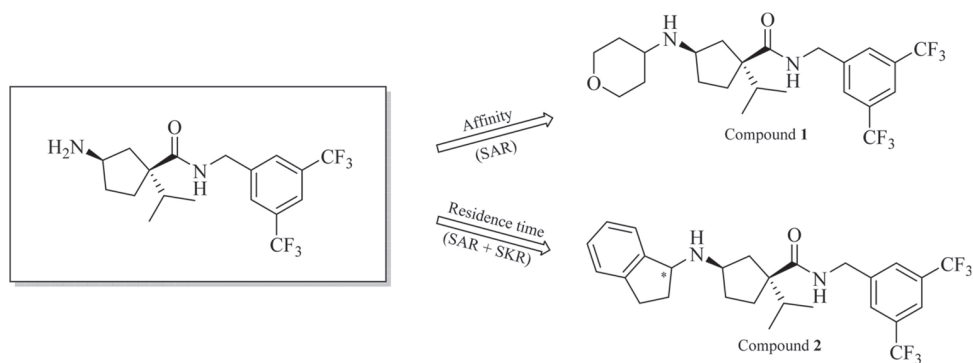

Fig. 2. RT and affinity values are both pharmacological parameters that may, however, suggest different lead structures.

Materials and Methods

Chemistry
Chemicals and reagents. All solvents and reagents were purchased from commercial sources and were of analytical grade. Demineralized water is simply referred to as H_2O, because it was used in all cases, unless stated otherwise (i.e., brine). ^1H and ^{13}C nuclear magnetic resonance (NMR) spectra were recorded on a Bruker AV 400 liquid spectrometer (^1H NMR, 400 MHz; ^{13}C NMR, 100 MHz) or using a Bruker 500 MHz Avance III NMR spectrometer (compounds **22a** and **22b**) at ambient temperature. Chemical shifts are reported in parts per million (ppm), are designated by δ, and are downfield to the internal standard tetramethylsilane (TMS). Coupling constants are reported in hertz and are designated as *J*. Analytical purity of the final compounds was determined by high-performance liquid chromatography (HPLC) with a Phenomenex Gemini 3 μm C18 110A column (50 × 4.6 mm,

3 μm), measuring UV absorbance at 254 nm. The sample preparation and HPLC method for compounds **1**, **2**, **7**–**9**, and **11**, **12** were as follows: 0.3–0.8 mg of compound was dissolved in 1 mL of a 1:1:1 mixture of $CH_3CN/H_2O/t$-BuOH and eluted from the column within 15 min at a flow rate of 1.0 mL. The elution method was set up as follows: 1–4 min isocratic system of $H_2O/CH_3CN/1\%$ TFA in H_2O, 80:10:10; from the 4th min, a gradient was applied from 80:10:10 to 0:90:10 within 9 min, followed by 1 min of equilibration at 0:90:10 and 1 min at 80:10:10. All compounds showed a single peak at the designated retention time and are at least 95% pure. High-resolution mass spectral analyses (HRMS) were performed on LTQ-Orbitrap FTMS operated in a positive ionization mode with an electrospray ionization (ESI) source, with the following conditions: mobile phase A, 0.1% formic acid in water; mobile phase B, 0.08% formic acid in CH_3CN; gradient, 10–80% B in 26 min; and flow rate, 0.4 mL/min. Preparative HPLCs (for compounds **10** and **13**–**32**) were performed on a Waters AutoPurification HPLC–ultraviolet (UV) system with a diode array detector using a Luna C18 Phenomenex column (75 × 30 mm, 5 μm), and a linear gradient from 1 to 99% of mobile phase B was applied. Mobile phase A consisted of 5 mM HCl solution, and mobile phase B consisted of acetonitrile. The flow rate was 50 mL/min. Liquid chromatography–mass spectrometry (LC–MS) analyses were performed using an Onyx C18 monolithic column (50 × 4.6 mm, 5 μm), and a linear gradient from 1 to 99% mobile phase B was applied. Mobile phase A consisted of 0.05% TFA in water, and mobile phase B consisted of 0.035% TFA in acetonitrile. The flow rate was 12 mL/min. Separations of enantiomers were accomplished using chiral SFC. The column was Phenomenex Lux-4 (250 × 10 mm, 5 μm). The mobile phase condition of 10% MeOH with 20 mM NH_3 and 90% CO_2 was applied at a flow rate of 10.0 mL/min. Optical rotations were measured on a Perkin-Elmer polarimeter in $CHCl_3$ at 20 °C. Thin-layer chromatography (TLC) was routinely consulted to monitor the progress of reactions, using aluminum-coated Merck silica gel F[254] plates. Purification by column chromatography was achieved by use of Grace Davison Davisil silica column material (LC60A, 30–200 μm). The procedure for a series of similar compounds is given as a general procedure for all within that series, annotated by the numbers of the compounds.

(1*S*,3*R*)-methyl-3-((tert-butoxycarbonyl)amino)-1-isopropylcyclopentanecarboxylate (3). Synthesis of (1*S*,3*R*)-methyl-3-((tert-butoxycarbonyl)amino)-1-isopropylcyclopentanecarboxylate (**3**) was achieved following the synthetic approach reported by Kothandaraman et al [15].

(1*S*,3*R*)-3-(*tert*-Butoxycarbonylamino)-1-isopropylcyclopentanecarboxylic Acid (4). A solution of ester **3** (4.20 g, 14.72 mmol) in EtOH (30 mL) and 4 M aqueous lithium hydroxide (LiOH aqueous, 40 mL) was refluxed for 4 h. After concentration in vacuum, the solution was acidified with aqueous hydrochloric acid and extracted with DCM/H_2O. The organic layer was dried over $MgSO_4$ and, after concentration in vacuum, yielded the desired product as a yellow powder (3.62 g, 91%). ^1H NMR (400 MHz, $CDCl_3$) δ: 10.75 (s, 1H), 6.53^a (s, 0.5H), 5.05^b (s, 0.5H), 3.98 – 3.78 (m, 1H), 2.25 – 1.50 (m, 7H), 1.40 (d, J = 16.8 Hz, 9H), 0.86 (d, J = 6.8 Hz, 6H); ^{13}C NMR (100 MHz, $CDCl_3$): δ 182.9^a, 181.7^b, 157.6^b, 155.6^a, 80.4^b, 79.1^a, 56.9, 52.8^b, 51.7^a, 38.6^b, 38.2^a, 35.0^b, 34.5^a, 33.2^a, 32.9^b, 32.1^a, 31.8^b, 28.3, 18.7, 18.2^b, 18.0^a. *a* and *b* are indicated for different rotamers.

tert*-Butyl(3-((3,5-bis(trifluoromethyl)benzyl)carbamoyl)-3-isopropylcyclopentyl) Carbamate (5). Compound **4** (1.53 g, 5.65 mmol) was dissolved in 50 mL of DCM. To this mixture 3,5 bis(trifluoromethyl) benzylamine (1.89 g, 5.65 mmol) was added with DiPEA (2.95 mL, 16.9 mmol), PyBrOP (2.64 g, 5.65 mmol), and DMAP (0.55 g, 4.5 mmol). The reaction mixture was stirred for 24 h at room temperature. The product was extracted with DCM/ citric acid solution in water and then with DCM/1 M NaOH. The organic layer was dried with $MgSO_4$ and evaporated. The product was purified by column chromatography (0–100% ethyl acetate in DCM) to give the product as a yellow oil (2.33 g, 83%). ^1H NMR (400 MHz, $CDCl_3$) δ: 7.69 (s, 3H), 7.25 (br s, 1H), 5.17 (br.s, 1H), 4.51–4.49 (m, 2H), 3.81 (br s, 1H), 1.99–1.90 (m, 4H), 1.69–1.72 (m, 2H), 1.50–1.58 (m, 1H), 1.36 (s, 9H), 0.74–0.77 (m, 6 H). ^{13}C NMR (100 MHz, $CDCl_3$) δ: 178.6, 155.6, 142.1, 132.2, 131.8, 131.5, 131.2, 127.4, 127.3, 124.5, 121.8, 121.0, 119.1, 78.9, 57.6, 51.6, 42.8, 36.3, 34.6, 33.3, 32.6, 28.2, 18.7, 17.5.

3-Amino-*N*-(3,5-bis(trifluoromethyl)benzyl)-1-isopropylcyclopentanecarboxamide (6). Trifluoroacetic acid (20 mL) was added to a solution of compound **5** (2.33 g, 4.6 mmol) in 50 mL of DCM. The reaction mixture was stirred for 1 h at room temperature. The reaction mixture was neutralized with 1 M NaOH and extracted with DCM. The organic layer was dried with $MgSO_4$, filtered, and evaporated to give the product as a yellow crystal (1.55 g, 85%). ^1H NMR (400 MHz, $CDCl_3$) δ: 9.16 (br s, 1H), 7.70–7.67 (m, 3H), 4.50–4.39 (m, 2H), 3.61–3.60 (m, 1H), 2.22–2.15 (m, 1H), 2.02–1.95 (m, 1H), 1.85–1.64 (m, 3H), 1.42–1.37 (m, 2H), 0.82–0.80 (m, 6H). ^{13}C NMR (100 MHz, $CDCl_3$) δ: 179.4, 142.5, 131.8, 131.5, 131.2, 130.9, 127.3, 127.2, 124.6, 121.9, 120.4, 119.2, 57.3, 52.2, 42.4, 39.7, 35.3, 33.9, 33.6, 18.8, 16.9.

General procedure for the synthesis of compounds 1, 2, and 11, 12. Amine **6** was dissolved in 4 mL of dichloroethane in a 5 mL reaction tube, and the corresponding ketone (1 equiv) was added. Sequentially, acetic acid (1 equiv) and sodium triacetoxyborohoydride (1.5 equiv) were added. The reaction mixture was stirred for 18 h at room temperature and then washed with 1 M NaOH and H_2O. The organic layer was dried with $MgSO_4$, filtered, and evaporated. The product was purified by column chromatography (0–100% ethyl acetate in DCM) to give the desired product.

(1*S*,3*R*)-*N*-(3,5-Bis(trifluoromethyl)benzyl)-1-isopropyl-3-((tetrahydro-2*H*-pyran-4-yl) amino)cyclopentanecarboxamide (1). Yield = 21%. ^{1}H NMR (400 MHz, CDCl$_3$) δ: 9.16 (s, 1H), 7.76–7.73 (m, 3H), 4.56–4.53 (m, 2H), 3.98–3.89 (m, 2H), 3.57–3.53 (m, 1H), 3.43–3.28 (m, 2H), 2.66–2.61 (m, 1H), 2.36–2.30 (m, 1H), 2.03–1.80 (m, 2H), 1.78–1.6 (m, 5H), 1.49–1.40 (m, 1H), 1.31–1.20 (m, 3H), 0.93–0.89 (m, 6H). ^{13}C NMR (400 MHz, CDCl$_3$) δ: 179.1, 142.4, 131.8, 131.54, 131.2, 130.9, 127.7, 127.3, 124.6, 121.8, 121.0, 119.2, 66.9, 66.9, 57.5, 54.8, 51.9, 42.6, 37.1, 35.1, 34.3, 33.7, 33.6, 33.3, 19.5, 17.0. LC–MS: 481[+]; t_R = 7.01 min.

(1*S*,3*R*)-*N*-(3,5-Bis(trifluoromethyl)benzyl)-3-((2,3-dihydro-1*H*-inden-1-yl)amino)-1-isopropylcyclopentanecarboxamide (2). Yield = 25% (mixture of diastereomers). ^{1}H NMR (400 MHz, CDCl$_3$) δ: 9.48 (s, 1H), 7.76–7.74 (m, 3H), 7.22–7.05 (m, 4H), 4.60–4.50 (m, 2H), 4.28–4.22 (m, 1H), 3.70–3.60 (m, 1H), 3.00–2.90 (m, 1H), 2.87–2.78 (m, 1H), 2.70–2.34 (m, 3H), 2.1–1.53 (m, 6H), 0.93–0.89 (m, 6H). ^{13}C NMR (400 MHz, CDCl$_3$) δ: 179.4, 144.5, 144.4, 144.6, 131.8, 131.5, 127.9, 127.6, 126.3, 126.2, 125.0, 123.5, 123.5, 122.0 121.9, 61.3, 58.0, 56.6, 42.6, 37.2, 36.0, 34.5, 33.9, 33.7, 33.4, 19.6, 17.0. LC–MS: 513[+]; t_R = 8.12 min.

General procedure for the synthesis of compounds 7–9. Amine **6** (1 equiv) was disolved in 4 mL of acetonitrile, and coresponding alkylating agent (1.2 equiv) was added. Sequentually, DiPEA (1.2 equiv) was added. The reaction mixture was stirred in a microwave for 2 h at 60 °C and purified with column chromatography (60% ethylacetate, 20% DCM, 20% petroleum ether, and 0–3% triethylamine in ethyl acetate).

(1*S*,3*R*)-3-(Benzylamino)-*N*-(3,5-bis(trifluoromethyl)benzyl)-1-isopropylcyclopentane-1-carboxamide (7). Yield = 27% (as HCl salt). ^{1}H NMR (400 MHz, CDCl$_3$) δ: 9.40 (br s, 1H), 7.73 (s, 1H), 7.66 (s, 2H), 7.30–7.24 (m, 3H), 7.16–7.13 (m, 2H), 4.44 (d, *J* = 4.8 Hz, 2H), 3.73 (d, *J* = 2.4 Hz, 2H), 3.46–3.41 (m, 1H), 2.41–2.33 (m, 1H), 2.02–1.90 (m, 4H), 1.85–1.78 (m, 2H), 1.59–1.52 (m, 1H), 0.91 (dd, *J*[1] = 10.8 Hz, *J*[2] = 6.8 Hz, 6H). ^{13}C NMR (100 MHz, CDCl$_3$) δ: 179.4,

142.6, 139.0, 132.0, 131.7, 131.3, 131.0, 128.6, 127.8, 127.5, 127.3, 124.6, 121.9, 120.8, 58.8, 58.7, 57.3, 51.9, 42.5, 35.3, 33.5, 33.1, 19.5, 16.9. LC–MS: 487$^+$; t_R: 7.40 min.

General procedure for the synthesis of compounds 10 and 13–32. To a series of 1.5 mL glass tubes was added amine **6** in NMP (0.95 M, 0.095 mmol), followed by solutions of different ketones (0.5 M, 0.1 mmol) in NMP, and these mixtures were subsequently treated with acetic acid (0.1 mmol), followed by 5-ethyl-2-methyl-pyridine borane (PEMB) (0.2 mmol). The reaction mixture was heated at 65 °C on a reaction block for 24 h. The reaction mixtures were purified directly using an automated mass-guided reverse-phase HPLC, and product-containing fractions were concentrated to give final products of >90% purity, as judged by LC–MS (average of 220 and 254 nm traces).

Biology

Chemicals and reagents. ^{125}I-CCL2 (2200 Ci/mmol) was purchased from Perkin-Elmer (Waltham, MA). INCB3344 was synthesized as described previously [16, 17]. [^{3}H]-INCB3344 (specific activity of 32 Ci mmol^{-1}) was custom-labeled by Vitrax (Placentia, CA), for which a dehydrogenated precursor of INCB3344 was provided. Tango CCR2-*bla* U2OS cells stably expressing human CCR2 were obtained from Invitrogen (Carlsbad, CA).

Cell culture and membrane preparation. U2OS cells stably expressing the human CCR2 receptor (Invitrogen, Carlsbad, CA) were cultured in McCoys5a medium supplemented with 10% fetal calf serum, 2 mM glutamine, 0.1 mM non-essential amino acids (NEAAs), 25 mM 4-(2-hydroxyethyl)piperazine-1-ethanesulfonic acid (HEPES), 1 mM sodium pyruvate, 100 IU/mL penicillin, 100 μg/mL streptomycin, 100 μg/mL G418, 50 μg/mL hygromycin, and 125 μg/mL zeocin in a humidified atmosphere at 37 °C and 5% CO_2. Cell culture and membrane preparation were performed as described previously [18].

^{125}I-CCL2 displacement assay. Binding assays were performed as described previously [18].

[^{3}H]-INCB3344 competition association assay. The kinetic parameters of unlabeled ligands at 25 °C were determined using the competition association assay described by Motulsky and Mahan [19]. At different time points, 10 μg of U2OS–CCR2 membranes was added to 1.8 nM [^{3}H]-INCB3344 in a total volume of 100 μL of assay buffer in the absence or presence of competing ligand. To validate the assay, three concentrations of INCB3344 (1-, 3-, and 10-fold its K_i value of [^{3}H]-INCB3344 displacement) were used. This validation

showed that using a single concentration (that equals the K_i) of unlabeled ligand was sufficient to accurately measure k_{on} and k_{off}. Incubation was terminated by dilution with ice-cold 50 mM tris(hydroxymethyl)aminomethane (Tris)-HCl buffer supplemented with 0.05% 3-[(3-cholamidopropyl)dimethylammonio]-1-propanesulfonate (CHAPS). Separation of bound from free radioligand was performed by rapid filtration through a 96-well GF/B filter plate pre-coated with 0.25% polyethylenimine (PEI) using a Perkin-Elmer FilterMate harvester (Perkin-Elmer, Groningen, Netherlands). Filters were washed 10 times with ice-cold wash buffer. A total of 25 μL of Microscint scintillation cocktail (Perkin-Elmer, Waltham, MA) was added to each well, and the filter-bound radioactivity was determined by scintillation spectrometry using the P-E 1450 Microbeta Wallac Trilux scintillation counter (Perkin-Elmer). Kinetic parameters of unlabeled ligands were calculated using eq 3, as mentioned below in the Data Analysis section.

[³H]-INCB3344 dual-point competition association assay. KRI values of unlabeled ligands were determined using the dual-point competition association assay as described previously, in which radioligand binding was determined at two different time points [20]. Time point t_1 represents the time at which radioligand binding reached 99.5% of total binding at equilibrium.

$$t_1 = 8 \cdot t_{1/2,association} \tag{1}$$

The second time point (t_2) was arbitrarily set at 4 h, where little but reliably measurable, specific binding remained. A total of 10 μg of U2OS–CCR2 membranes were incubated for 50 min (t_1) or 240 min (t_2) in a total volume of 100 μL of assay buffer with 1.8 nM [³H]-INCB3344 in the absence or presence of unlabeled ligands at 25 °C. The amount of radioligand bound to the receptor was measured after co-incubation of the unlabeled ligands at 1-fold their respective K_i value in the ^{125}I-CCL2 displacement assay. Incubations were terminated, and samples were obtained as described under the [³H]-INCB3344 Competition Association Assay section. KRI values of unlabeled ligands were calculated using eq 2, as mentioned below in the Data Analysis section.

Data analysis. All experiments were analyzed using the nonlinear regression curve fitting program Prism 5 (GraphPad, San Diego, CA). For radioligand displacement data, K_i values were calculated from IC_{50} values using the Cheng and Prusoff equation [21]. Data of the dual-point competition association assay were analyzed as described previously [20].

KRI values were calculated by dividing the specific radioligand binding measured at t_1 (B_{t1}) by its binding at t_2 (B_{t2}) in the presence of unlabeled competing ligand as follows:

$$KRI = B_{t1} / B_{t2} \tag{2}$$

Association and dissociation rates for unlabeled ligands were determined by nonlinear regression analysis of the competition association data as described by Motulsky and Mahan [19]

$$
\begin{aligned}
K_A &= k_1[L] \cdot 10^{-9} + k_2 \\
K_B &= k_3[I] \cdot 10^{-9} + k_4 \\
S &= \sqrt{(K_A - K_B)^2 + 4 \cdot k_1 \cdot k_3 \cdot L \cdot I \cdot 10^{-18}} \\
K_F &= 0.5(K_A + K_B + S) \\
K_S &= 0.5(K_A + K_B - S) \\
Q &= \frac{B_{max} \cdot k_1 \cdot L \cdot 10^{-9}}{K_F - K_S} \\
Y &= Q \cdot \left(\frac{k_4 \cdot (K_F - K_S)}{K_F \cdot K_S} + \frac{k_4 - K_F}{K_F} e^{(-K_F \cdot X)} - \frac{k_4 - K_S}{K_S} e^{(-K_S \cdot X)} \right)
\end{aligned}
\tag{3}
$$

where X is the time (min), Y is the specific binding (disintegrations per minute (DPM)), k_1 is k_{on} (M^{-1} min^{-1}) of [^{3}H]-INCB3344 predetermined in association experiments, k_2 is k_{off} (min^{-1}) of [^{3}H]-INCB3344 predetermined in dissociation experiments, L is the concentration of [^{3}H]-INCB3344 used (nM), B_{max} is the total binding (DPM), and I is the concentration of unlabeled ligand (nM). Fixing these parameters into eq 3 allows for the following parameters to be calculated: k_3 is k_{on} (M^{-1} min^{-1}) of the unlabeled ligand, and k_4 is k_{off} (min^{-1}) of the unlabeled ligand. The association and dissociation rates were used to calculate the "kinetic K_D" as follows:

$$K_D = k_{off} / k_{on} \tag{4}$$

The RT was calculated according to the formula RT = $1/k_{off}$.

Results and discussion

Chemistry. Synthesis of (1*S*,3*R*)-methyl-3-((tert-butoxycarbonyl)amino)-1-isopropylcyclopentanecarboxylate (**3**) was achieved following the synthetic approach reported by Kothandaraman et al. [15]. The desired *N-tert*-butyloxycarbonyl (Boc)-protected ester **3** was saponified to yield acid **4**. Subsequently, acid **4** was used in the peptide-coupling reaction with 3,5-bis(trifluoromethyl)benzylamine to yield amide **5** under bromo-tris-pyrrolidino phosphoniumhexafluorophosphate (PyBroP) conditions [22]. Removal of the *N*-Boc group with trifluoroacetic acid (TFA) in dichloromethane (DCM) produced amine **6**. Reductive amination with different ketones under NaBH(AcO)$_3$ conditions afforded the desired products **1**, **2**, and **11**, **12**. Compounds **7**–**9** were synthesized by alkylating amine **6** with different alkylating agents. Compounds **10** and **13**–**32** were generated from amine **6** and an array of different ketones with 5-ethyl-2-methylpyridine borane complex (PEMB) under conditions reported by Burkhardt and Coleridge (Scheme 1) [23].
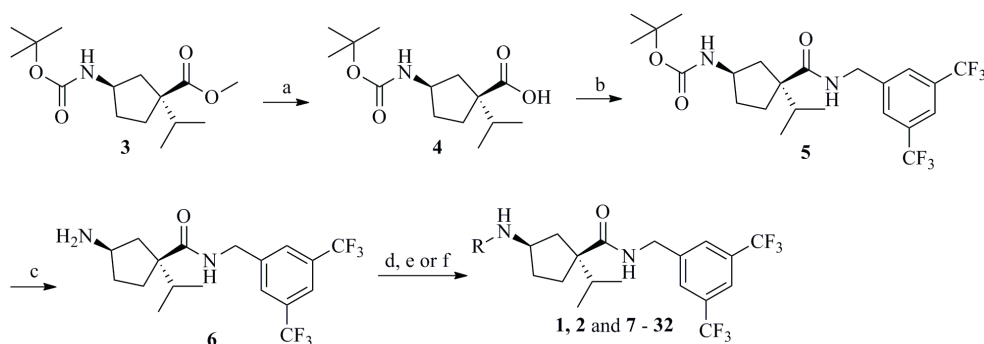
Scheme 1. Synthesis of CCR2 antagonists. Reagents and conditions: (a) 4 M LiOH aqueous, MeOH, reflux, 4 h, 91%; (b) 3,5-bis(trifluoromethyl)benzylamine, PyBrOP, N,N-diisopropylethylamine (DiPEA), N,N-dimethylaminopyridine (DMAP), DCM, room temperature, 24 h, 83%; (c) TFA, DCM, room temperature, 1 h, 85%; (d) corresponding ketone, (AcO)$_3$BHNa, AcOH, DCE, room temperature, 18 h, 21–86% (compounds 1, 2, and 11, 12); (e) corresponding alkylating agent, DiPEA, CH$_3$CN, 60 °C, 2 h, 14–54% (compounds 7–9); (f) for array synthesis, corresponding ketone, 5-ethyl-2-methylpyridine borane (PEMB), AcOH, N-methylpyrrolidone (NMP), 65 °C, 24 h (compounds 10 and 13–32).

Biology. To determine the binding affinity, all compounds were tested in a ^{125}I-CCL2 displacement assay on human bone osteosarcoma (U2OS)–CCR2 membrane preparations as described previously by our group [18]. Several methods can be used to determine ligand binding kinetics (e.g., a kinetic radioligand binding assay [24], surface plasmon resonance (SPR) [25], "two-step" competition binding assay [26], and "Tag-lite" Cisbio [27]). Most of these assays require special modifications of the target protein or the ligand. Therefore, we

chose to use the competition association assay, because this assay allowed us to determine the kinetics of unlabeled ligands to the receptor expressed in membrane preparations. In our hands, this is the most robust and accurate assay to measure kinetics of unlabeled ligands.

Validation of the [³H]-INCB3344 competition association assay for CCR2. A competition association assay was set up to determine the kinetic parameters of unlabeled ligands [19]. For this assay, we used the radiolabeled small-molecule CCR2 antagonist [³H]-INCB3344 [28], instead of the endogenous agonist protein radioligand ^{125}I-CCL2. Because of the large size of CCL2 (8600 Da), there is at best only a partial overlap in the binding site with small-molecule antagonists. Because the theoretical model of the competition association assay is based on the assumption that unlabeled and radiolabeled ligands should compete for the same binding site, we decided to use [³H]-INCB3344 in our assay. This radioligand bears considerable chemical resemblance to the compounds reported in this study. We first validated this method by measuring the competition association of [³H]-INCB3344 in the absence and presence of three different concentrations of INCB3344 (1-, 3-, and 10-fold its K_i) (Fig. 3). This resulted in k_{on} and k_{off} values for unlabeled INCB3344 of 0.035 ± 0.010 nM^{-1} min^{-1} and 0.024 ± 0.002 min^{-1}, respectively, at 25 °C (Table 1). The corresponding RT was 43 ± 2 min. These results were in good agreement with k_{on} and k_{off} values of [³H]-INCB3344 binding from "traditional" association and dissociation experiments, 0.054 ± 0.002 nM^{-1} min^{-1} and 0.013 ± 0.002 min^{-1}, respectively [18] (Table 1).
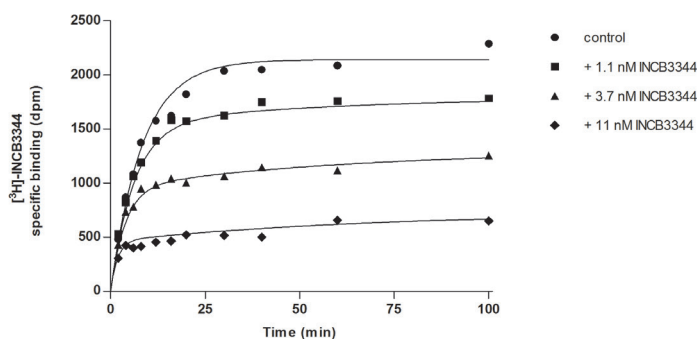

Fig. 3. Competition association assay with [³H]-INCB3344 at 25 ºC in the absence or presence of 1.1, 3.7 and 11 nM unlabeled INCB3344.

Table 1. Comparison of equilibrium binding and kinetic parameters of INCB3344 determined using different methods

assay	K_D/K_i (nM)	k_{on} ($nM^{-1} min^{-1}$)	k_{off} (min^{-1})
saturation binding[a]	0.90 ± 0.03	NA^b	NA
displacement[c]	1.2 ± 0.1	NA	NA
association and dissociation[d]	0.23 ± 0.04	0.054 ± 0.002	0.013 ± 0.002
competition association[e]	0.72 ± 0.19	0.035 ± 0.010	0.024 ± 0.002

Data are presented as mean ± S.E.M. of three independent experiments performed in duplicate.
[a]Saturation binding of 1- 45 nM [^{3}H]-INCB3344 to CCR2 at 25 ºC.
[b]NA = not applicable.
[c]Displacement of 3.5 nM [^{3}H]-INCB3344 from CCR2 at 25 ºC.
[d]Association and dissociation of [^{3}H]-INCB3344 measured in standard kinetic assays at 25 ºC.
[e]Association and dissociation of INCB3344 measured in competition association assays at 25 ºC.

Screening of CCR2 antagonists using the dual-point competition association assay. The competition association assay described above is laborious and time-consuming, and hence, we developed a so-called dual-point competition association assay for CCR2, according to principles that we recently established for the adenosine A_1 receptor [20]. To this end, we co-incubated [^{3}H]-INCB3344 with unlabeled antagonists at a concentration equal to their K_i value that was determined in the ^{125}I-CCL2 displacement assay. The so-called kinetic rate index (KRI) was calculated by dividing the specific radioligand binding at 50 min (t_1) by the binding at 240 min (t_2). In this assay, antagonists with a slower dissociation rate and, therefore, a longer RT than [^{3}H]-INCB3344 would result in a KRI > 1 (Fig. 4).
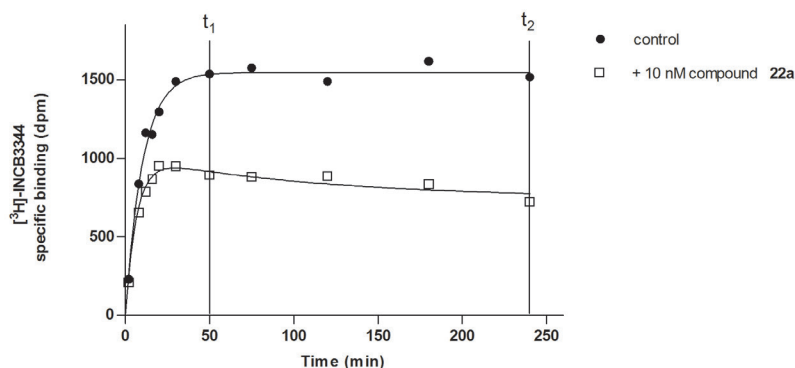

Fig. 4. Representative competition association curves of control and long-residence-time compound **22a**. B_{t1}, specific radioligand binding at the first time point (t_1 = 50 min); B_{t2}, specific radioligand binding at the second time point (t_2 = 240 min). KRI is defined as B_{t1}/B_{t2}, which equaled 1.2 for compound **22a**.

Structure–affinity relationships (SARs) versus structure–RT relationships

The 3-amino-1-isopropylcyclopentanecarboxamide scaffold has been extensively evaluated on the basis of binding affinities for CCR2 and selectivity against other chemokine receptors and the human ether-à-go-go-related gene (hERG) channel [15, 29, 30]. Therefore, we decided to resynthesize several reported derivatives of compound **1** [15, 31] and determine their binding affinity in radioligand displacement assays (Table 2). Introduction of the benzyl group yielded compound **7** with an affinity of 437 nM. When the spacer length between the phenyl ring and basic nitrogen was extended to ethyl, binding was almost lost (compound **8**; K_i = 2400 nM). Prolonging the chain to propyl allowed us to regain affinity (compound **9**; K_i = 134 nM). Combining the knowledge of compounds **7** and **9** in one structure yielded the indane derivative compound **2** with even more improved affinity (K_i = 50 nM). Expanding the ring system to tetrahydronaphthalene resulted in an additional increase in affinity (compound **10**; K_i = 33 nM). Removal of aromatics yielded compound **11** with a cyclohexane ring, which showed a decrease in affinity (K_i = 110 nM), but incorporation of heteroatoms in the 4 position regained affinity (compounds **1** and **12**; K_i = 6.8 and 31 nM, respectively) as described by Kothandaraman et al. [15]. On the basis of affinity alone, compound **1** would be the logical choice for lead optimization, which yielded the clinical candidate MK-0812 in the case of the Merck research group [10]. However, the kinetic evaluation of these known structures in a competition association assay allowed us to use an additional parameter, RT. In this assay, the best affinity compound **1** had a RT of 2.4 min, while compound **2** had a 4-fold longer RT of 9.5 min (Table 2). Structurally closely related compound **10** had a RT of 5.6 min, which convinced us to continue with compounds **2** and **10**, because they had a longer RT.

Table 2. Binding affinities and residence time (RT) of compounds **1**, **2**, **7 – 12**.
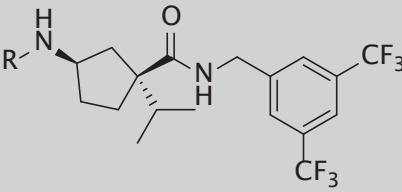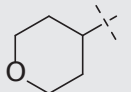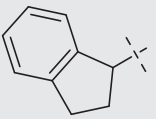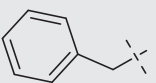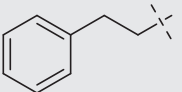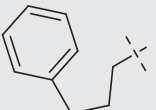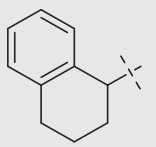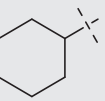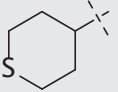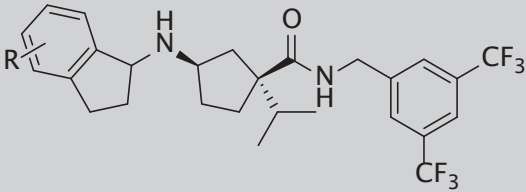

Nr.	R	K_i (nM) ± S.E.M. (n=3)	RT (min)
1		6.8 ± 2.2	2.4 ± 0.2
2		50 ± 8	9.5 ± 1.5
7		437 ± 62	-
8		2400 ± 900	-
9		134 ± 35	-
10		33 ± 2	5.6 ± 0.5
11		110 ± 13	1.9 ± 0.4
12		31 ± 9	4.3 ± 1.4

Table 3. Binding affinities and KRI of indenyl derivatives **2** and **13 − 28**.

Nr.	R	K_i (nM) ± SEM (n=3)	KRI (n=2)
2	H	50 ± 8	0.7 (0.7/0.7)
13	4-NH$_2$	43 ± 7	0.8 (0.7/0.8)
14	4-OH	86 ± 8	0.6 (0.5/0.8)
15	4-CN	70 ± 11	0.8 (0.7/0.8)
16	4-Me	26 %[a]	-
17	4-OMe	30 %[a]	-
18	5-OMe	6.1 ± 0.7	0.6 (0.6/0.6)
19	5-OH	29 ± 2	0.7 (0.7/0.8)
20	5-F	30 %[a]	-
21	5-Cl	18 ± 1	1.1 (1.1/1.2)
22	5-Br	7.2 ± 0.5	1.1 (1.0/1.1)
23	6-Cl	28 %[a]	-
24	6-Me	55 ± 2	0.8 (0.8/0.8)
25	6-CN	54 ± 4	0.6 (0.6/0.6)
26	4;5-di-OMe	130 ± 6	-
27	5;6-di-OMe	3.9 ± 0.3	0.7 (0.7/0.7)
28	5;6-(-OCH$_2$O-)	6.3 ± 0.8	0.6 (0.6/0.7)

[a]Percent displacement at 1μM ^{125}I-CCL2.

Using a number of commercially available indanones, we introduced different substituents on the indane ring (Table 3) to cover chemical space as broadly as possible. The SAR exploration on the 4 position showed that H-bond-accepting and hydrophilic groups are tolerated. The 4-NH$_2$ group led to a minor increase (compound **13**; K_i = 43 nM), but 4-OH and 4-CN groups showed a decrease in affinity (compounds **14** and **15**; K_i = 86 and 70 nM, respectively). 4-Me (compound**16**) and 4-MeO (compound **17**) were not tolerated on this position (26 and 30% displacement at 1 μM, respectively). On the 5 position, methoxy and hydroxyl groups improved the affinity, which had also been suggested for other
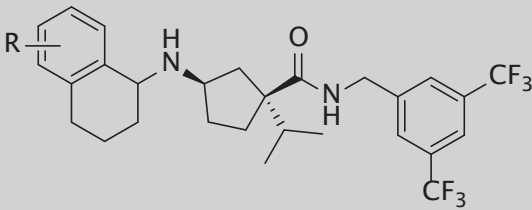
CCR2 antagonists [30, 32]. The methoxy group (compound **18**) showed an 8-fold increase in affinity (6.1 nM), while the hydroxyl group (compound **19**) displayed a less than 2-fold increase compared to the unsubstituted indenyl derivative (29 and 50 nM, respectively). On the contrary, the introduction of fluorine, which was previously reported as the best substituent in arylpiperidine analogues by Pasternak et al. [30], resulted in a dramatic decrease in affinity in the case of the indenyl derivative (compound**20**; 30% displacement at 1 μM). 5-Cl substitution yielded better affinity than 5-F (compound **21**; 18 nM), and 5-Br was better than 5-Cl (compound **22**; 7.2 nM). 6-Cl (compound **23**) led to a dramatic decrease in affinity (28% displacement at 1 μM). However, 6-Me and 6-CN groups were tolerated, having similar affinities to the unsubstituted indane ring (compounds **24** and **25**; K_i = 55 and 54 nM, respectively).

We continued the investigation with the analysis of disubstitution, learning that the combination of 4,5 substitution resulted in more than a 2-fold decrease in affinity (compound**26**; K_i = 130 nM). On the contrary, the 5,6-dimethoxy group yielded compound **27** with a high affinity of 3.9 nM. Connecting the dimethoxy groups into a dioxolane ring yielded a small decrease in affinity (compound **28**; K_i = 6.3 nM).

Using the knowledge of the best position for substitution, we continued the investigation on the 1,2,3,4-tetrahydronaphthalene ring by introducing substituents on the 5 position (Table 4). Electron-donating groups showed very similar results to what we found for the indenyl moiety. Compounds **29** and **30** showed good affinity (27 and 35 nM, respectively), while electron-withdrawing groups showed a decrease or complete lack of affinity (compounds **31** and **32**).
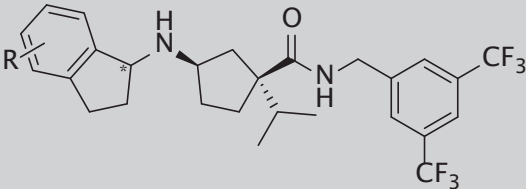
After SAR evaluation, the higher affinity compounds were screened in our kinetic assay to determine their KRI value [20] (see also Figure 2). A KRI value of <1 indicates that the RT of a tested compound is shorter than the RT of the radioligand (less than 43 min in this particular case). A KRI value of >1 reflects a RT of more than 43 min.

6

Table 4. Binding affinities and KRI of tetrahydronaphthalene derivatives **10** and **29 – 32**.

Nr.	R	K_i (nM) ± SEM (n=3)	KRI
10	H	33 ± 2	0.6 (0.6/0.5)
29	5-OMe	27 ± 1	0.7 (0.7/0.8)
30	5-OH	35 ± 2	0.8 (0.7/0.8)
31	5-Br	48%[a]	-
32	5-COOH	0%[a]	-

[a]Percent displacement at 1 μM ^{125}I-CCL2.

Compound **2** in the screen showed a KRI value of 0.7 (RT = 9.5 min). However, compounds **21** and **22** had higher KRI values (1.1 for both compounds). These compounds were tested in a full competition association assay to determine their association and dissociation rate constants (Table 5). Increasing the size of the substituent, change from 5-Cl to 5-Br (compound **21** versus compound **22**), also yielded longer RTs (56 and 94 min, respectively). Compound **22** was separated in two diastereomers by preparative supercritical fluid chromatography (SFC) using a Phenomenex Lux-4 column (Phenomenex, Inc.). The first compound to elute (**22a**) had an affinity of 3.6 nM. However, the second compound (**22b**) to elute had a 100-fold decreased affinity (K_i = 289 nM). These separated diastereomers had very similar k_{off} rates (Table 5), which translated to similar RTs (compound **22a**, RT = 135 min; compound **22b**, RT = 77 min), but a significant difference was observed for their k_{on} rates. Apparently, the stereochemistry of the indane ring system has a major impact on the compound association rate to the receptor, while the dissociation is not affected.

Table 5. Kinetic data of compounds **21**, **22**, **22a** and **22b**.

Nr.	R	K_i (nM) ± SEM (n=3)	k_{on} (nM^{-1} min^{-1})	k_{off} (min^{-1})	RT (min)
21	5-Cl	18 ± 1	0.0027 ± 0.0006	0.020 ± 0.004	56 ± 14
22	5-Br	7.2 ± 0.5	0.010 ± 0.002	0.011 ± 0.0002	94 ± 3
22a	5-Br	3.6 ± 0.9	0.0053 ± 0.0007	0.0074 ± 0.0004	135 ± 8
22b	5-Br	289 ± 94	0.00030 ± 0.00007	0.015 ± 0.004	77 ± 18

Conclusion

We have demonstrated that, next to affinity, additional knowledge of the RT is useful for selecting and developing new CCR2 antagonists. (1*S*,3*R*)-*N*-(3,5-Bis(trifluoromethyl)benzyl)-3-((5-bromo-2,3-dihydro-1*H*-inden-1-yl)amino)-1-isopropylcyclopentanecarboxamide (**22a**) had a RT of 135 min. In comparison to the best affinity compound from the first SAR screening, i.e., compound **1** (Table 1), compound **22a** had a 56-fold increased RT while having similar affinity. This indicates that affinity and RT do not correlate; moreover, while SAR driven hit-to-lead optimizations often fail in later stages of drug development because of the lack of efficacy (e.g., MK-0812), it has been shown on other targets that RT is linked to the duration of the *in vivo* antagonist effect [33-35]. Compound **22a** may thus be a useful tool to test whether prolonged blockade of CCR2 has a beneficial effect on CCR2-related disorders, such as neuropathic pain.

6

References

1. Charo, I.F. and R.M. Ransohoff, *The many roles of chemokines and chemokine receptors in inflammation.* The New England journal of medicine, 2006. 354(6): p. 610-21.

2. Serbina, N.V. and E.G. Pamer, *Monocyte emigration from bone marrow during bacterial infection requires signals mediated by chemokine receptor CCR2.* Nat Immunol, 2006. 7(3): p. 311-317.

3. Leuschner, F., et al., *Therapeutic siRNA silencing in inflammatory monocytes in mice.* Nat Biotechnol, 2011. 29(11): p. 1005-10.

4. Fife, B.T., et al., *CC chemokine receptor 2 is critical for induction of experimental autoimmune encephalomyelitis* J Exp Med, 2000. 192(6): p. 899-905.

5. Dawson, T.C., et al., *Absence of CC chemokine receptor-2 reduces atherosclerosis in apolipoprotein E-deficient mice.* Atherosclerosis, 1999. 143(1): p. 205-11.

6. Ogata, H., et al., *The role of monocyte chemoattractant protein-1 (MCP-1) in the pathogenesis of collagen-induced arthritis in rats* J Pathol, 1997. 182(1): p. 106-14.

7. Kanda, H., et al., *MCP-1 contributes to macrophage infiltration into adipose tissue, insulin resistance, and hepatic steatosis in obesity.* J Clin Invest, 2006. 116(6): p. 1494-505.

8. Kim, Y.K., et al., *Association between a genetic variation of CC chemokine receptor-2 and atopic asthma.* Allergy, 2007. 62(2): p. 208-9.

9. White, F.A., P. Feldman, and R.J. Miller, *Chemokine Signaling and the Management of Neuropathic Pain.* Mol Interv, 2009. 9(4): p. 188-195.

10. Struthers, M. and A. Pasternak, *CCR2 antagonists.* Curr Top Med Chem, 2010. 10(13): p. 1278-98.

11. Swinney, D.C., *Biochemical mechanisms of drug action: what does it take for success?* Nat Rev Drug Discov, 2004. 3(9): p. 801-808.

12. Copeland, R.A., D.L. Pompliano, and T.D. Meek, *Drug-target residence time and its implications for lead optimization.* Nat Rev Drug Discov, 2006. 5(9): p. 730-9.

13. Zhang, R.M. and F. Monsma, *Binding kinetics and mechanism of action: toward the discovery and development of better and best in class drugs.* Exp Opin Drug Discov, 2010. 5(11): p. 1023-1029.

14. Copeland, R.A., *Evaluation of enzyme inhibitors in drug discovery. A guide for medicinal chemists and pharmacologists.* Methods Biochem Anal, 2005. 46: p. 1-265.

15. Kothandaraman, S., et al., *Design, synthesis, and structure-activity relationship of novel CCR2 antagonists.* Bioorg Med Chem Lett, 2009. 19(6): p. 1830-4.

16. Xue, C.M., B.; Feng, H.; Cao, G.; Huang, T.; Zheng, C.; Robinson, D. J.; Han, A., *3-Aminopyrrolidine derivatives as modulators of chemokine receptors.* Patent WO2004050024, June 17, 2004.

17. Brodmerkel, C.M., et al., *Discovery and pharmacological characterization of a novel rodent-active CCR2 antagonist, INCB3344.* J Immunol, 2005. 175(8): p. 5370-8.

18. Zweemer, A.J.M., et al., *Multiple Binding Sites for Small-Molecule Antagonists at the CC Chemokine Receptor 2.* Mol Pharmacol, 2013. 84(4): p. 551-561.

19. Motulsky, H.J. and L.C. Mahan, *The kinetics of competitive radioligand binding predicted by the law of mass action.* Mol Pharmacol, 1984. 25(1): p. 1-9.

20. Guo, D., et al., *Dual-Point Competition Association Assay: A Fast and High-Throughput Kinetic Screening Method for Assessing Ligand-Receptor Binding Kinetics.* J Biomol Screen, 2013. 18(3): p. 309-320.

21. Cheng, Y. and W.H. Prusoff, *Relationship between Inhibition Constant (K1) and Concentration of Inhibitor Which Causes 50 Per Cent Inhibition (I50) of an Enzymatic-Reaction.* Biochem Pharmacol, 1973. 22(23): p. 3099-3108.

22. Frerot, E., et al., *Pybop and Pybrop - 2 Reagents for the Difficult Coupling of the Alpha,Alpha-Dialkyl Amino-Acid, Aib.* Tetrahedron, 1991. 47(2): p. 259-270.

23. Burkhardt, E.R. and B.M. Coleridge, *Reductive amination with 5-ethyl-2-methylpyridine borane.* Tetrahedron Lett, 2008. 49(35): p. 5152-5155.

24. Casarosa, P., et al., *Functional and biochemical rationales for 24-h long duration of action of olodaterol.* J Pharmacol Exp Ther, 2011. 377: p. 600-609.

25. Rich, R.L., et al., *Kinetic analysis of estrogen receptor/ligand interactions.* Proc Natl Acad Sci U S A, 2002. 99(13): p. 8562-7.

26. Packeu, A., et al., *Estimation of the dissociation rate of unlabelled ligand-receptor complexes by a 'two-step' competition binding approach.* Br J Pharmacol, 2010. 161(6): p. 1311-28.

27. *http://www.htrf.com/tag-lite-technology.*

28. Shin, N., et al., *Pharmacological characterization of INCB3344, a small molecule antagonist of human CCR2.* Biochem Biophys Res Comm, 2009. 387(2): p. 251-5.

29. Yang, L., et al., *Discovery of 3-piperidinyl-1-cyclopentanecarboxamide as a novel scaffold for highly potent CC chemokine receptor 2 antagonists.* J Med Chem, 2007. 50(11): p. 2609-11.

30. Pasternak, A., et al., *Potent heteroarylpiperidine and carboxyphenylpiperidine 1-alkyl-cyclopentane carboxamide CCR2 antagonists.* Bioorg Med Chem Lett, 2008. 18(3): p. 994-8.

31. Goble, S.D., et al., *Alkylamino, arylamino, and sulfonamido cyclopentyl amide modulators of chemokine receptor activity.* U.S. Patent 2007/117797, May 24, 2007.

32. Zhang, X., et al., *Overcoming hERG activity in the discovery of a series of 4-azetidinyl-1-aryl-cyclohexanes as CCR2 antagonists.* Bioorg Med Chem Lett, 2011. 21(18): p. 5577-82.

33. Van Liefde, I. and G. Vauquelin, *Sartan-AT1 receptor interactions: in vitro evidence for insurmountable antagonism and inverse agonism.* Mol Cell Endocrinol, 2009. 302(2): p. 237-43.

34. Casarosa, P., et al., *Preclinical evaluation of long-acting muscarinic antagonists: comparison of tiotropium and investigational drugs.* J Pharmacol Exp Ther, 2009. 330(2): p. 660-8.

35. Anthes, J.C., et al., *Biochemical characterization of desloratadine, a potent antagonist of the human histamine H(1) receptor.* Eur J Pharmacol, 2002. 449(3): p. 229-37.

6